Electromagnetically pumped free-electron laser with a guide magnetic field

A. Goldring and L. Friedland
Center for Plasma Physics, Racah Institute of Physics, Hebrew University of Jerusalem, Jerusalem, Israel
(Received 12 February 1985)

The operation of a free-electron laser with an electromagnetic pump in the presence of a guide magnetic field is considered. It is shown that several different steady-state helical equilibria are allowed in a given configuration of the pump and guide fields. The study of the dynamics of the beam shows that the helical equilibrium is an exception rather than the rule. Thus only special initial conditions and careful tapering of the transition region at the entrance into the laser allow launching the beam on one of the stable steady states. The small signal gain in the laser is also derived. It is shown that the gain can be substantially enhanced when the beam approaches the orbital instability regime. Numerical examples demonstrate that the strength of the pump field in these conditions can be greatly reduced while still providing enhanced gain in the laser.

I. INTRODUCTION

Conventional free-electron lasers exploit relativistic electron beams propagating along periodic transverse magnetostatic structures (a wiggler). Such a configuration is capable of amplifying electromagnetic radiation of frequency $f \sim \gamma^2 k_w c/\pi$ (for $\gamma \gg 1$) where $\gamma = [1-(v/c)^2]^{-1/2}$ is the relativistic factor of the electron beam and $k_w = 2\pi/\lambda_w$ represents the wave vector associated with the period λ_w of the magnetostatic pump "wave." Unfortunately, technical reasons put an upper limit on k_w, which usually does not exceed ~ 3 cm^{-1}, thus limiting the frequency of the laser to $f \sim 30\gamma^2$ (GHz).

A natural way of further increasing the laser frequency, for a given value of γ, is to exploit an electromagnetic wave as a pump instead of the wiggler. The lack of a coherent tunable intense radiation source for operation of the laser in the attractive subcentimeter regime prevents simple implementation of the idea of the electromagnetic pump. Nonetheless, various solutions to the problem have been suggested in the literature. The two-stage free-electron-laser approach[1] is the most developed at present. In this type of laser a conventional wiggler-based free-electron laser, in the first stage, generates an intense electromagnetic wave, which in turn, in the second stage, serves as a pump for possibly the same electron beam. Similar ideas have been implemented recently by Carmel *et al.*,[2] who demonstrated the first operation of a two-stage backward-wave free-electron laser.

In addition to the possibility of a significant increase of k_w, there exists an additional advantage in the use of the electromagnetic pump. It is due to the fact that the wiggler field $\mathbf{B}_w$ has a simple periodic one-dimensional structure only on the axis of the wiggler. Away from the axis, for radii $r \gtrsim 1/k_w$, the radial dependence of $\mathbf{B}_w$, due to the magnetostatic requirement $\nabla \times \mathbf{B}_w = 0$, effectively worsens the quality of the electron beam. Thus, only beams with relatively small radii can be employed in conventional free-electron lasers. In contrast, in the case of an electromagnetic pump $\nabla \times \mathbf{B}$ is balanced by the displacement current, allowing, in principle, propagation of purely one-dimensional waves in large interaction volumes. In practice, however, finite dimensions of the pump source may impose radial limitations. In free space, for example, these radial effects are due to diffraction and are dictated by the geometry of the source and the length of the interaction region. These radial limitations, however, are less severe for shorter wavelengths of the pump, in contrast to the case of the wiggler.

The object of the present study is to explore the idea of the use of an electromagnetic pump in free-electron lasers, which employ additional guide magnetic fields. The presence of the latter is a necessity in intense ($I > 1$ kA) relatively low-energy ($\gamma < 10$) electron-beam experiments as, for example, the one discussed in Ref. 2. It is known[3] that in conventional free-electron lasers, the guide fields lead to a variety of nontrivial consequences. For example, simple stable helical electron trajectories in combined crossed magnetostatic pump and guide fields are rather exceptional. Moreover, several different classes of helical orbits are allowed by the system for a given magnetostatic field configuration. Also, an attractive possibility of an enhancement of the small signal gain in the laser exists[4] at much lower magnitudes of the pump field than in the laser without the guide field. It is a primary goal of this work to find and exploit the parallels to all these effects in free-electron lasers with an electromagnetic pump. Several steps towards achieving this goal have been reported in the literature. Sprangle *et al.*[5] describe collective interaction between radiation and cold magnetized electron beams in helical equilibrium. Enhanced growth rates are reported when the frequency of the pump in the beam frame approaches the electron-cyclotron frequency. Later, Ref. 6 mentions that in the case of a slow pump wave ($v_p/c = \omega/ck_w < 1$) one can make a coordinate transformation to the system moving with the phase velocity of the pump wave. In such a coordinate system the pump becomes purely magnetostatic, thus allowing the use of the conventional theory for combined wiggler and guide field free-electron laser. Gell *et al.*[7] recently described magnetized electron-beam dynamics in an arbitrary strength luminous ($v_p = c$) electromagnetic wave.

Several recent studies by Stenflo *et al.*[8–10] deal with a general theory of stability and radiation of guided electron beams in a large-amplitude circularly polarized wave.

These studies assume a helical beam equilibrium without further investigation of the question of its existence and stability against perturbations in initial conditions and ways of experimental implementation of the stable helical equilibria. No attempt was made, so far, to calculate the expected small signal gain in the laser with electromagnetic pump and guide magnetic fields.

The present work comprises a comprehensive theoretical investigation of all the above-mentioned issues. The paper is organized as follows: Sec. II describes the dynamics of relativistic electron beams in combined guide and electromagnetic pump fields. Possible helical, steady-state equilibria are also discussed in this section. In Sec. III the stability of the helical equilibria is studied, and possible ways of launching the beam into one of these steady states are discussed. In Sec. IV we develop a formalism for the calculation of the small signal gain in the laser. Finally, in Sec. V, we present a numerical example and further discuss the advantages and limitations of the proposed laser configuration.

II. HELICAL BEAM EQUILIBRIUM

Consider a cold relativistic electron beam propagating in the z direction in an electromagnetic field given by

$$\mathbf{E}_0=-\frac{1}{c}\frac{\partial \mathbf{A}_0}{\partial t},\quad \mathbf{B}_0=\nabla\times\mathbf{A}_0+B_1\hat{\mathbf{e}}_z\ , \tag{1}$$

where $B_1=\text{const}$ and

$$\mathbf{A}_0=-A_0[\cos(k_0z-\omega_0t)\hat{\mathbf{e}}_x+\sin(k_0z-\omega_0t)\hat{\mathbf{e}}_y]\ . \tag{2}$$

We assume that the density of the beam is low enough and does not influence $\mathbf{E}_0$ and $\mathbf{B}_0$. Equation (2) describes a variety of electromagnetic waves encountered in many experimental situations. For instance, circularly polarized electromagnetic waves represented by (2) with $k_0c/\omega_0<1$ are characteristic for axial regions in circular metal waveguides. The situation when $k_0c/\omega_0>1$ can be achieved by using various slowing-down structures in the waveguides. Alternatively, magnetized streaming plasmas can support both slow and fast waves described by Eq. (2) with various dispersion characteristics. Also, the case $k_0c=\omega_0$ represents a vacuum wave and the situation $\omega_0=0$, describes the conventional magnetostatic field on the axis of a magnetic wiggler widely employed in free-electron lasers.

The dynamics of the electron beam in our case is described by the momentum equation

$$\left[\frac{\partial}{\partial t}+\mathbf{v}\cdot\nabla\right](m\gamma\mathbf{v})=-e(\mathbf{E}_0+\mathbf{v}\times\mathbf{B}_0/c)\ , \tag{3}$$

which, on using (1), can also be written as

$$\left[\frac{\partial}{\partial\tau}+\mathbf{u}\cdot\nabla\right](\gamma\mathbf{u}-\boldsymbol{\alpha})=\Omega\hat{\mathbf{e}}_z\times\mathbf{u}-(\nabla\boldsymbol{\alpha})\cdot\mathbf{u}\ , \tag{4}$$

where we are using the following notations: $\tau=ct$, $\mathbf{u}=\mathbf{v}/c$, $\boldsymbol{\alpha}=e\mathbf{A}_0/mc^2$, and $\Omega=eB_1/mc^2$.

Define the following orthonormal set of base vectors:

$$\begin{aligned}\hat{\mathbf{e}}_1&=-\hat{\mathbf{e}}_x\sin\phi+\hat{\mathbf{e}}_y\cos\phi\ ,\\ \hat{\mathbf{e}}_2&=-\hat{\mathbf{e}}_x\cos\phi-\hat{\mathbf{e}}_y\sin\phi\ ,\\ \hat{\mathbf{e}}_3&=\hat{\mathbf{e}}_z\ ,\end{aligned} \tag{5}$$

where $\phi=k_0z-\omega_0t$. Then $\boldsymbol{\alpha}=eA_0/mc^2\hat{\mathbf{e}}_2=\alpha_0\hat{\mathbf{e}}_2$ and if we define $\omega_0'=\omega_0/c$, Eq. (4), in components, becomes

$$\left[\frac{\partial}{\partial\tau}+u_3\frac{\partial}{\partial z}\right](\gamma u_1)+(\omega_0'-u_3k_0)(\gamma u_2-\alpha_0)=-\Omega u_2\ , \tag{6}$$

$$\left[\frac{\partial}{\partial\tau}+u_3\frac{\partial}{\partial z}\right](\gamma u_2)-(\omega_0'-u_3k_0)(\gamma u_1)=\Omega u_1\ , \tag{7}$$

$$\left[\frac{\partial}{\partial\tau}+u_3\frac{\partial}{\partial z}\right](\gamma u_3)=k_0\alpha_0u_1\ . \tag{8}$$

Note that Eqs. (6)–(8) have a particular solution: $u_1=u_{10}=0$, $u_2=u_{20}=\text{const}$, $u_3=u_{30}=\text{const}$, $\gamma=\gamma_0=\text{const}$, where

$$u_{20}=\frac{(k_0u_{30}-\omega_0')\alpha_0/\gamma_0}{k_0u_{30}-\omega_0'-\Omega/\gamma_0} \tag{9}$$

and

$$1/\gamma_0^2=1-u_{20}^2-u_{30}^2\ . \tag{10}$$

In the following we will refer to the helical electron trajectories described by Eqs. (9) and (10) as the steady-state solutions.

Substitution of (9) and (10) yields a fourth-order polynomial for u_{30}, describing four possible steady-state solutions for given γ_0, α_0, Ω, k_0, and ω_0'. Figures 1 and 2

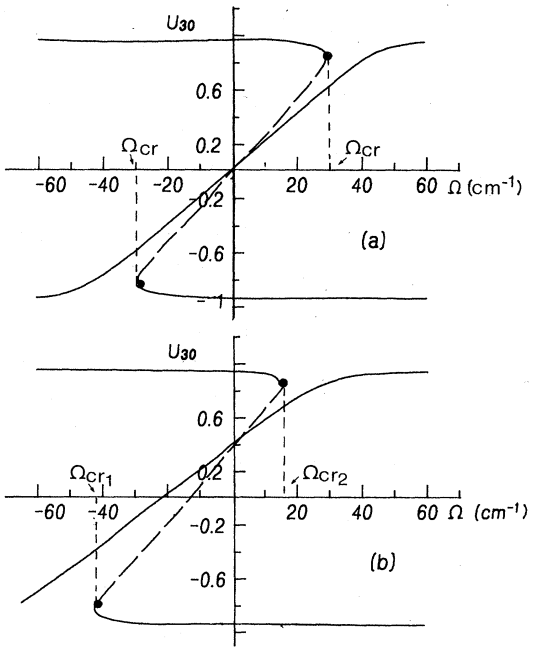

FIG. 1. Steady-state axial velocity u_{30} vs Ω. (a) $v_p=0$. (b) $v_p=0.4$. In all the cases, $\gamma_0=3$, $k_0=15\ \text{cm}^{-1}$, and $\alpha_0=0.3$.

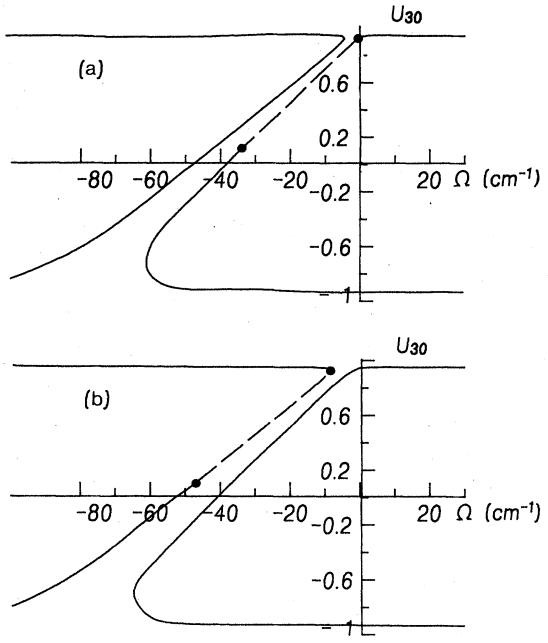

FIG. 2. Steady-state axial velocity u_{30} vs Ω. (a) $v_p=0.95$. (b) $v_p=1.05$. In all the cases $\gamma_0=3$, $k_0=15$ cm^{-1}, and $\alpha_0=0.3$.

show these solutions versus Ω for the case $\alpha_0=0.3$, $\gamma_0=3$, $k_0=15$ cm^{-1}, and different values of the reduced phase velocity of the wave $v_p=\omega_0'/k_0=0$, 0.4, 0.95, and 1.05. The solution, antisymmetric around $\Omega=0$, in the case $v_p=0$ [Fig. 1(a)], corresponds to a previously studied case of the magnetic wiggler,[3,4,6] where four solutions for u_{30} exist when $|\Omega|<\Omega_{cr}$. Only two real solutions for u_{30} are present, however, when $|\Omega|>\Omega_{cr}$. The situation becomes more complex when $v_p\neq 0$. Hence, as can be seen in Figs. 1(b), 2(a), and 2(b), the solution $u_{30}=u_{30}(\Omega)$ loses its symmetry and only for $\Omega=0$ does it have a simple form $u_{30}=v_p\pm[1-(\alpha_0^2+1)/\gamma_0^2]^{1/2}$. Two different critical values of Ω ($\Omega_{cr_1},\Omega_{cr_2}$) exist at which $du_{30}/d\Omega=\infty$ and two real branches of the steady states disappear. An additional interesting feature of the steady states in the case $v_p\neq 0$ is, that for $v_p=[1-(\alpha_0^2+1)/\gamma_0^2]^{1/2}$ there exist three coinciding solutions for u_{30} at $\Omega=0$, and when $v_p>[1-(\alpha_0^2+1)/\gamma_0^2]^{1/2}$, the topology of the branches changes with two simply connected pairs of solutions above and below the line $k_0u_{30}-\omega_0'-\Omega/\gamma_0=0$, for $\Omega<\Omega_{cr_1}$ and $\Omega>\Omega_{cr_2}$, respectively [Figs. 2(a) and 2(b)].

We will show in Sec. IV that one can considerably enhance the single-particle gain in a free-electron laser operating in the helical beam equilibria, described here, if Ω approaches its critical values. In addition we will demonstrate later that the critical values play an important role in trying to experimentally launch the beam on one of the stable equilibria. Therefore, in the rest of this section we will derive a simple equation for Ω_{cr}. The basic equation describing the axial velocity of the beam in the steady states is [see Eqs. (9) and (10)]

$$1-u_{30}^2-[(k_0u_{30}-\omega_0)\alpha_0/a\gamma_0]^2=1/\gamma_0^2 , \tag{11}$$

where we defined $a=k_0u_{30}-\omega_0'-\Omega/\gamma_0$. Assume existence of a solution $u_{30}=u_{30}(\Omega)$ of Eq. (11). In substituting this solution back into Eq. (11) and differentiating the resulting equality with respect to Ω we find after some algebra

$$\frac{du_{30}}{d\Omega}=-\frac{\alpha_0^2(k_0u_{30}-\omega_0')^2}{au_{30}\gamma_0^3\mu_0^2} , \tag{12}$$

where

$$a\mu_0^2=a^3-k_0^2\alpha_0^2\Omega(1-v_p/u_{30})/\gamma_0^3 . \tag{13}$$

The critical values of Ω are thus described by the condition

$$\mu_0^2=a^2-\frac{\alpha_0^2(k_0u_{30}-\omega_0')k_0\Omega}{u_{30}\gamma_0^3a}=0 . \tag{14}$$

Further simplification is possible by rewriting Eq. (11) as

$$a=(k_0u_{30}-\omega_0')\alpha_0/(1-1/\gamma_0^2-u_{30}^2)^{1/2}\gamma_0 , \tag{15}$$

and using the expression

$$\Omega/\gamma_0=-a+k_0u_{30}-\omega_0' . \tag{16}$$

Substitution of (15) and (16) into (14), after some algebra, finally yields an algebraic equation for the values of $u_{30}=u_{cr}$ at $\Omega=\Omega_{cr}$ as follows:

$$\alpha_0(1-1/\gamma_0^2-u_{cr}v_p)=\gamma_0(1-1/\gamma_0^2-u_{cr}^2)^{3/2} . \tag{17}$$

When u_{cr} is found from Eq. (17) we can get Ω_{cr} by employing Eqs. (16) and (15). A simple expression for u_{cr}

$$u_{cr}^2=1-1/\gamma_0^2-[\alpha_0(1-1/\gamma_0^2)/\gamma_0]^{2/3} \tag{18}$$

can be found from (17), in the conventional magnetostatically pumped ($v_p=0$) free-electron laser. Note also, that it follows from (17) that $u_{cr}=v_p$, if $v_p^2=1-(1+\alpha_0^2)/\gamma_0^2$ in accordance with the previously mentioned possibility, occurring at $\Omega=0$.

III. STABILITY ANALYSIS

At this stage we consider a perturbed steady-state helical equilibrium. Write the solutions of Eqs. (6)–(8) in the form

$$u_i=u_{i0}+w_i,\quad i=1,2,3 . \tag{19}$$

If the perturbations w_i are small enough, they obey the following linearized equations:

$$\dot{w}_1=aw_2-(k_0u_{20}-k_0\alpha_0/\gamma_0)w_3 +(k_0u_{30}-\omega_0')u_{20}g/\gamma_0 , \tag{20}$$

$$\dot{w}_2=-aw_1-u_{20}g/\gamma_0 , \tag{21}$$

$$\dot{w}_3=k_0\alpha_0w_1/\gamma_0-u_{30}g/\gamma_0 , \tag{22}$$

where the dots describe the time derivative along the electron trajectory and $g=\gamma-\gamma_0$ is associated with the perturbation in energy. The energy equation is

$$mc^2\dot{\gamma} = -e\mathbf{E}_0\cdot\mathbf{v} \tag{23}$$

yielding

$$\dot{g} = \omega_0'\alpha_0 w_1 \ . \tag{24}$$

We now differentiate Eq. (20) with respect to time and substitute Eqs. (21), and (22), and (24) in the resulting equation. This leads to

$$\ddot{w}_1 + \mu_s^2 w_1 = 0 \ , \tag{25}$$

where

$$a\mu_s^2 = a^3 - k_0^2\alpha_0^2\Omega(1-v_p^2)/\gamma_0^3 \ . \tag{26}$$

Thus, the necessary condition for the stability of the steady-state helical trajectory is $\mu_s^2 > 0$. The regions of the unstable helical equilibria are shown in Fig. 1 by the dashed lines.

Consider now the problem of experimentally achieving one of the stable steady states. These stable helical electron orbits are rather exceptional and obviously require special entrance conditions of the electron beam into the interaction region.

Ideally, one has to launch a cold electron beam prepared to be initially in one of the steady states and adiabatically switch on the pump field along the trajectory in the transition region of the laser, so that the electron will adiabatically follow the helical equilibrium until it enters the homogeneous part of the interaction space. Experimentally, the pump field may be mostly z dependent but slowly fall radially as one moves away from the axis. Then adiabatic switching on of the pump is achieved by launching the beam at a small angle to the axis from the pump-field-free region. Alternatively, by using quasioptical cavities or waveguides with variable cross sections we can taper the z dependence of the pump field and launch the beam along the axis.

Note, that it follows from (9) that when $\alpha_0 \to 0$ we have $u_{20}=0$ and therefore, a natural way of launching the beam into a steady state is to prepare it initially to have purely axial velocity. In the rest of Sec. III we will consider only these particular initial conditions. In Fig. 2 we show an example of launching the beam onto one of the steady states. We employed $\alpha(z)=\alpha_0[1-\exp(-\delta z)]$ with $\delta=0.1\ \mathrm{cm}^{-1}$, $k_0=15\ \mathrm{cm}^{-1}$, $\Omega=-50\ \mathrm{cm}^{-1}$, $\alpha_0=0.3$, and $v_p=-0.95$. Note that in this example $u_{30}<0$, namely the beam is propagating in the direction, opposite to the direction of propagation of the pump wave. Figure 3 shows the adiabatic decrease of the beam axial velocity u_3 in the transition region and achievement of the constant steady-state value in the homogeneous region ($z > 1/\delta$). At the same time the transverse velocity component u_1 remains small and u_2 starts from zero and reaches its steady-state value of 0.24 in the homogeneous region. The small oscillations are due to the transition region and have frequency μ_s [see Eq. (25)].

An additional effect we found in this example, was a slight increase of the γ factor while passing the transition region. In order to arrive at the steady state shown in Fig. 3 with $\gamma_0=3$, we launched the beam with an initial value of $\gamma=2.97$.

As it also happens in conventional free-electron lasers

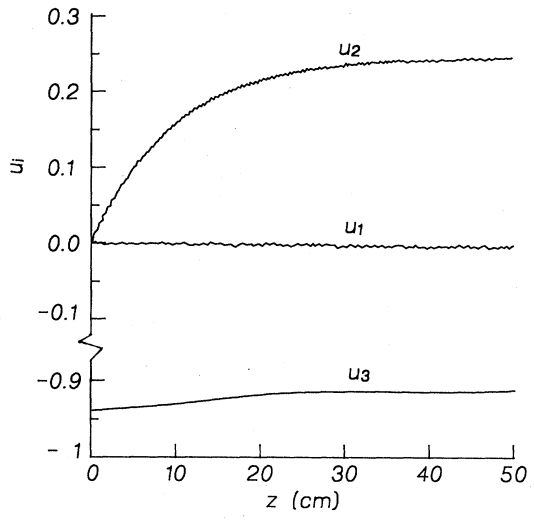

FIG. 3. Spatial evolution of the components of the electron velocity in launching the beam into a steady state. The parameters in the homogeneous region are $\gamma_0=3$, $k_0=15\ \mathrm{cm}^{-1}$, $\alpha_0=0.3$, $v_p=-0.95$, $\Omega=-50\ \mathrm{cm}^{-1}$.

with a guide magnetic field,[3] the adiabaticity of the transition region and the aforementioned initial conditions are not sufficient for achieving the steady state in the homogeneous region. Indeed, while passing the transition region, electrons adiabatically following the steady state, may encounter a point z_0 at which the local guide field is critical for the corresponding set of values of $\alpha_0(z)$, $k_0(z)$, and $\gamma_0(z)$. At such a point $\mu_0=0$ [see definition in Eq. (13), and therefore $du_{30}/d\alpha_0 \sim (\mu_0)^{-1}$ becomes infinite]. The corresponding real branch of the solutions for u_{30} disappears when $\alpha_0(z) > \alpha_0(z_0)$ and an adiabatic transition to another branch is impossible since it requires a jump in u_{30}. As a result, the beam departs from the steady state and its motion becomes rather complex.

This situation is demonstrated in Fig. 4 where all the initial parameters are the same as in Fig. 3 except

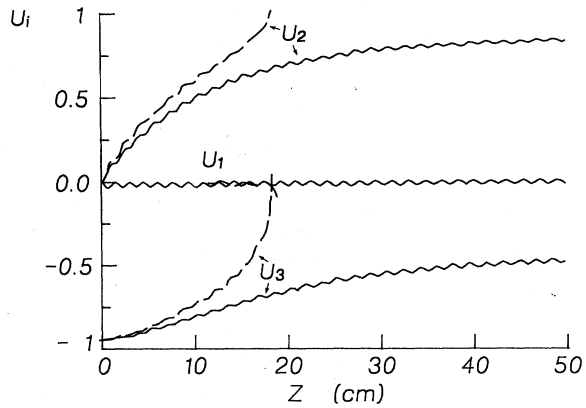

FIG. 4. Evolution of the velocity components in the vicinity of orbital instability. In the homogeneous region $k_0=15\ \mathrm{cm}^{-1}$, $\alpha_0=0.3$, $v_p=-0.95$, $\Omega=-73\ \mathrm{cm}^{-1}$ (solid lines), and $\Omega=-74\ \mathrm{cm}^{-1}$ (dashed lines).

$\Omega=-73$ cm^{-1} (solid lines) and $\Omega=-74$ cm^{-1} (dashed lines). One can see in Fig. 3 the transition to instability at $\Omega=-74$ cm^{-1}, where u_1, u_2, and u_3 vary rapidly with z, from $z=15$ cm and on, inside the transition region.

It is interesting to note that in contrast to the case where $\Omega=-50$ cm^{-1} (Fig. 3) the beam experiences a considerable acceleration in the transition region. For example, the final value of γ_0 in Fig. 4 for the case of $\Omega=-74$ cm^{-1} was 5.4 (while initially $\gamma_0=2.97$).

Thus, in conclusion, in launching the beam adiabatically in transition regions into one of the steady states, one should avoid conditions where the local value of μ_0 becomes small. In these regions, the stability of the beam is very sensitive to perturbations in initial conditions. Nevertheless, we will see in the next section that operation of the free-electron laser in the regime in which both stability parameters μ_s and μ_0 are small in the homogeneous region of the interaction, allows to enhance the small signal gain in the laser.

IV. SMALL SIGNAL GAIN

Consider a configuration in which, in addition to the pump electromagnetic wave $\mathbf{E}_0$, $\mathbf{B}_0$ we introduce another small-amplitude plane vacuum electromagnetic wave $\mathbf{E}=\hat{\mathbf{e}}_x E\cos(kz-\omega t+\alpha)$, $\mathbf{B}=\hat{\mathbf{e}}_z\times\mathbf{E}$ characterized by its frequency ω and $k=\omega/c$. Conventionally, the small signal single-particle gain in such a system is associated with the average electron-energy change over a given distance L, of the interaction region, with the averaging taken over an ensemble of electrons entering the interaction region at different random time moments. Since, usually, the gain is proportional to E^2, typically, classical small signal gain calculations require perturbation analysis of the equations of motion up to the second order in E. Such calculations, in the presence of the guide field tend to be algebraically rather complex.[4] Therefore, here, we are adopting a different recent approach,[11] which is based on the use of the correspondence principle and requires only the first-order perturbation analysis. The new method was successful in calculating the gain in a variety of free-electron-laser configurations,[11,12] including the laser with a magnetostatic wiggler and guide fields, which is a special case of a system considered here ($\omega_0=0$). It was shown in Ref. 11 that the gain is given by

$$\Gamma=-\frac{(\hbar\omega)^2 N_e}{Q}\frac{d}{d\epsilon}(u_{30}\langle n\rangle_{\mathrm{av}}) , \tag{27}$$

where $Q=E^2/8\pi$ is the time-averaged energy density of the perturbing electromagnetic wave, N_e is the particle density of the electron beam, $\epsilon=mc^2\gamma_0$ is the energy of the electrons, and $\langle n\rangle_{\mathrm{av}}$ is the average number of quanta $\hbar\omega$ absorbed by an electron in a single pass through the interaction region. One can find $\langle n\rangle_{\mathrm{av}}$ from[11]

$$\langle n\rangle_{\mathrm{av}}=\langle s^2\rangle_{\mathrm{av}}/2(\hbar\omega)^2 \tag{28}$$

where s is given by

$$s=-ec\int_{t_1}^{t_2}\mathbf{u}(t')\cdot\{\mathbf{E}_0[z(t'),t']+\mathbf{E}[z(t'),t']\}dt' , \tag{29}$$

where the integration is with respect to the time t' along the electron trajectory and t_1 and t_2 are the moments at which the electron enters and leaves the interaction region. We now assume that without the perturbation $\mathbf{E}$, $\mathbf{B}$ the electrons move on one of the steady-state helical trajectories, described in Sec. II, and subsequently write $\mathbf{u}$ in (29) as $\mathbf{u}=\mathbf{u}_0+\mathbf{w}$, so that correct to first order in E

$$s=-ec\left[\int_{t_1}^{t_2}(\mathbf{u}_0\cdot\mathbf{E})dt+\int_{t_1}^{t_2}(\mathbf{w}\cdot\mathbf{E}_0)dt\right] . \tag{30}$$

It is interesting to note that the second integral in (30) is missing in magnetostatically pumped free-electron lasers, where $\mathbf{E}_0=0$.

Consider now the first integral in (30)

$$\begin{aligned} I_1&=-ec\int_{t_1}^{t_2}dt'\mathbf{u}_0\cdot\mathbf{E} \\ &=+ecu_{20}E\int_{t_1}^{t_2}\cos(k_0z-\omega_0t') \\ &\quad\times\cos(kz-\omega t'+\alpha)dt' . \end{aligned} \tag{31}$$

Correct to the lowest significant order in (31) we can write $z=z_0+u_{30}\tau''$, where $\tau''=\tau'-\tau_1-T/2$, so that

$$\begin{aligned} I_1=eu_{20}E\int_{-T/2}^{T/2}&\cos[(k_0u_{30}-\omega_0')\tau''+\phi_1] \\ &\times\cos[(ku_{30}-\omega')\tau''+\psi]d\tau'' , \end{aligned} \tag{32}$$

where $T=L/u_{30}$ is the reduced time duration of the interaction in a region of length L, $\omega'=\omega/c$, $\phi_1=-\omega_0'T/2-\omega_0'\tau_1+k_0z_0$, $\psi=-\omega_0'T/2-\omega'\tau_1=kz_0+\alpha$, and z_0 is the center of the interaction region. Finally, the integration in (32) yields

$$\begin{aligned} I_1=eu_{20}E\left[\frac{\sin(\beta_1T/2)}{\beta_1}\cos(\phi_1-\psi)\right. \\ \left.+\frac{\sin(\beta_2T/2)}{\beta_2}\cos(\phi_1+\psi)\right] , \end{aligned} \tag{33}$$

where

$$\beta_1=(k-k_0)u_{30}-(\omega'-\omega_0') ,$$

$$\beta_2=(k+k_0)u_{30}-(\omega'+\omega_0') .$$

Consider the case when $\beta_1\simeq 0$, or (since $\omega'=|k|$)

$$\omega'\simeq\frac{\omega_0'-k_0u_{30}}{1-u_{30}\mathrm{sgn}(k)}\simeq 2\gamma_0^2(\omega_0'-k_0u_{30}) . \tag{34}$$

For $k_0<0$ (the pump wave propagates in the direction opposite to the direction of propagation of the beam), we deal with the double Doppler upshifted frequency of the pump, characteristic to free-electron lasers. For these conditions, $|\beta_2|\simeq 2|\omega_0'-k_0u_{30}|\gg\beta_1$, and consequently we can neglect the second term in Eq. (33).

Next, we consider the second integral in (30),

$$I_2=-ec\int_{t_1}^{t_2}\mathbf{w}\cdot\mathbf{E}_0dt'=-eA_0\omega_0\int_{t_1}^{t_2}w_1dt' . \tag{35}$$

In order to find the perturbation w_1 due to the amplified wave, we go back to the momentum equations (20)—(22) and add new electromagnetic interaction terms. This results in

$$\dot{w}_1 = a w_2 - (k_0 u_{20} - k_0 \alpha_0/\gamma_0) w_3 + (k_0 u_{30} - \omega_0') u_{20} g/\gamma_0 + \epsilon_1 (u_{30}-1)/\gamma_0 ,$$
$$\dot{w}_2 = -a w_1 - u_{20} \dot{g}/\gamma_0 + \epsilon_2 (u_{30}-1)/\gamma_0 , \quad (36)$$
$$\dot{w}_3 = k_0 \alpha_0 w_1/\gamma_0 - u_{30} \dot{g}/\gamma_0 - \epsilon_2 u_{20}/\gamma_0 ,$$

where

$$\epsilon_1 = \frac{e}{mc^2} \hat{\mathbf{e}}_1 \cdot \mathbf{E} = -\frac{eE}{mc^2} \cos(kz - \omega' \tau + \alpha) \sin(k_0 z - \omega_0' \tau) , \quad (37)$$
$$\epsilon_2 = \frac{e}{mc^2} \hat{\mathbf{e}}_2 \cdot \mathbf{E} = -\frac{eE}{mc^2} \cos(kz - \omega' \tau + \alpha) \cos(k_0 z - \omega_0' \tau) ,$$

and in contrast to (24)

$$\dot{g} = \omega_0' \alpha_0 W_1 - \epsilon_2 u_{20} . \quad (38)$$

As in Eq. (33), we can now neglect the rapidly oscillating part in (37) and write approximately

$$\epsilon_1 \simeq -\frac{eE}{2mc^2} \sin[(k-k_0)z - (\omega' - \omega_0')\tau + \alpha] \simeq \frac{eE}{2mc^2} \sin(\beta_1 \tau'' + \phi_1 - \psi) ,$$
$$\epsilon_2 \simeq -\frac{eE}{2mc^2} \cos[(k-k_0)z - (\omega' - \omega_0')\tau + \alpha] \simeq \frac{eE}{2mc^2} \cos(\beta_1 \tau'' + \phi_1 - \psi) , \quad (39)$$

where, similar to (32), $-T/2 < \tau'' < T/2$, and ϕ_1 and ψ are defined as in (33). Now we differentiate the first equation in (36) with respect to τ and substitute in the resulting equation, expressions for w_2 and w_3 from Eq. (36) and Eq. (38) for g. This yields

$$\ddot{w}_1 + \mu_s^2 w_1 = A \epsilon_2 , \quad (40)$$

where, as could be expected, μ_s^2 is the stability parameter [see (26)] and A is given by

$$A = \frac{1}{\gamma_0} \left[(1-u_{30})(a+\beta_1) + \frac{\Omega u_{20}^2}{\gamma_0} \frac{1-v_p}{u_{30}-v_p} \right] . \quad (41)$$

Next, we solve Eq. (40) subject to the initial conditions

$$w_1(\tau_1) = 0, \quad \dot{w}_1(\tau_1) = r ,$$
$$w_1(\tau'') = \frac{r}{\mu_s} \sin\left[\mu_s \left[\tau'' - \frac{T}{2}\right]\right] + \frac{\beta_1 A \epsilon_0}{2\mu_s(\mu_s^2 - \beta_1^2)} \sin(\beta_1 \tau_1 + \delta) \sin[\mu_s(\tau - \tau_1)] - \frac{A\epsilon}{2(\mu_s^2 - \beta_1^2)} \cos(\beta \tau_1 + \delta) \cos[\mu_s(\tau - \tau_1)] + \frac{A\epsilon_0}{2(\mu_s^2 - \beta_1^2)} \cos(\beta_1 \tau + \phi_1 - \psi) , \quad (42)$$

where $\epsilon_0 = eE/mc^2$. This solution can be simplified if, consistently with (34), we require $\beta_1 \to 0$ (and $\mu_s^2 \gg \beta_1^2$). Then, on retaining in (42) only the low-frequency variation, we have

$$w_1(\tau'') \simeq \frac{A\epsilon_2}{2\mu_s^2} \cos(\beta_1 \tau'' + \phi_1 - \psi) . \quad (43)$$

Thus, after the integration (35) becomes

$$I_2 = \frac{e\alpha_0 \omega_0 A E}{\mu_s^2 c} \frac{\sin(\beta_1 T/2)}{\beta_1} \cos(\phi_1 - \psi) \quad (44)$$

and therefore

$$s = I_1 + I_2 = \frac{LE}{2u_{30}} \left[e u_{20} + \frac{e\alpha_0 \omega_0 A}{\mu_s^2 c} \right] \frac{\sin\theta}{\theta} \cos(\Phi - \Psi) , \quad (45)$$

where $\theta = \beta_1 T/2 \simeq \beta_1 L/2$. Substitution of (45) into (28) and averaging over τ, then yields

$$\langle n \rangle_{\text{av}} = \frac{\pi Q}{2(\hbar\omega)^2} \left[u_{20} + \frac{\alpha_0 \omega_0 A}{\mu_s^2 c} \right]^2 \left[\frac{eL}{u_{30}} \right]^2 F(\theta) , \quad (46)$$

with $F(\theta) = [(\sin\theta)/\theta]^2$. This expression can now be substituted into Eq. (27) for the gain

$$\Gamma = -\tfrac{1}{2} \pi N_e \frac{d}{d\epsilon} \left[\frac{(eL)^2}{u_{30}} \left[u_{20} + \frac{\alpha_0 \omega_0 A}{c\mu_s^2} \right]^2 \right] F(\theta) . \quad (47)$$

We will now make the usual assumption in the theory of free-electron lasers, that the main contribution from the differentiation with respect to ϵ in Eq. (47) comes from the differentiation of $F(\theta)$. Indeed, since $\theta = \beta_1 L/2u_{30}$ we have $dF/d\epsilon \sim L$ and therefore it leads to the only contribution in Γ proportional to L^3. Neglecting for large L the terms of the order L^2 in the gain, we have

$$\Gamma \simeq -\frac{\pi N_e e^2}{2u_{30}} L^2 \left[u_{20} + \frac{\alpha_0 \omega_0 A}{c\mu_s^2} \right]^2 \frac{dF}{d\theta} \frac{d\theta}{d\epsilon} = -\frac{\pi N_e e^2}{4u_{30}^3} L^3 \left[u_{20} + \frac{\alpha_0 \omega_0 A}{c\mu_s^2} \right]^2 \frac{dF}{d\theta} \frac{du_{30}}{d\epsilon} (\omega' - \omega_0') . \quad (48)$$

Finally, Eq. (11) yields

$$\frac{du_{30}}{d\epsilon} = \frac{a^3 + k_0^3 (u_{30} - v_p)^3 \alpha_0^2}{u_{30} \mu_0^2 mc^2 \gamma_0^3 a} \quad (49)$$

and therefore the gain formula becomes

$$\Gamma = -\frac{\pi N_e e^2 L^3 (\omega' - \omega_0')}{4mc^2 \gamma_0^3 u_{30}^4 \mu_0^2 a} \left[u_{20} + \frac{\alpha_0 \omega_0 A}{c\mu_s^2} \right]^2 \times [a^3 + k_0^3 (u_{30} - v_p)^3 \alpha_0^2] \frac{dF}{d\theta} . \quad (50)$$

Note that it follows from (50) that operation of the laser in the regime in which u_0 or μ_s, or both are small, may enhance the gain. This is due to the enhanced response of the system to perturbations while approaching the unstable situation. We will demonstrate this phenomenon in a numerical example in the Sec. V.

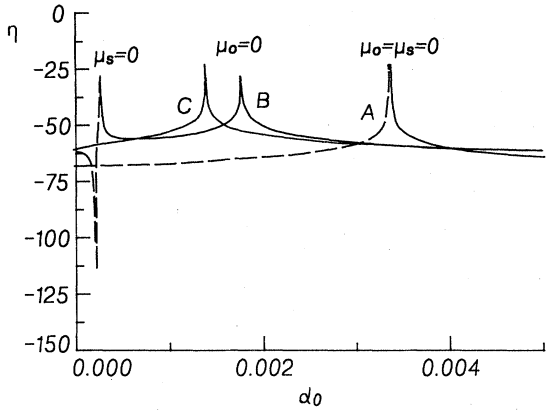

FIG. 5. Gain parameter η vs the strength of the pump field. A, conventional wiggler ($v_p=0$). B, $v_p=0.85$. C, $v_p=1.30$. In all cases $\gamma_0=3$, $L=100$ cm, $|u_\perp|=0.1$, and $\omega'=180$ cm^{-1}. The dashed parts of the curves indicate unstable orbital regime.

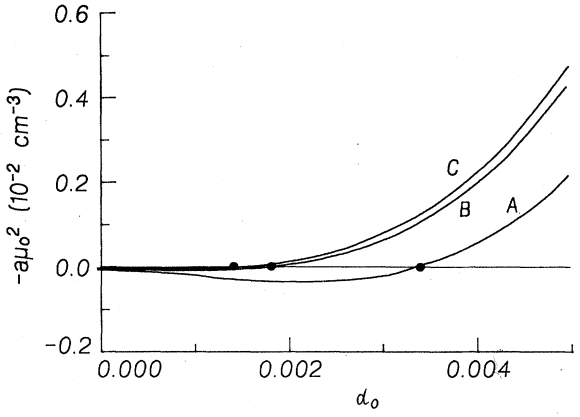

FIG. 6. Orbital stability parameter $a\mu_0^2$ vs α_0 for conditions of Fig. 5. A, $v_p=0$. B, $v_p=0.85$. C, $v_p=1.30$.

V. NUMERICAL EXAMPLE AND CONCLUSIONS

In this section we compare performance of two free-electron-laser amplifiers both capable of amplifying radiation of the same frequency. The first is the conventional magnetostatically pumped free-electron laser and the second is the laser with the electromagnetic pump, discussed in the previous sections. Consider the case where in both lasers $\gamma_0=3$, $L=100$ cm, $|u_\perp|=0.1$, and the frequency of the amplified radiation is $\omega'=180$ cm^{-1} ($f\simeq 10^{12}$ Hz). We also assume that the strength of the pump field α_0 in the lasers is the same. With all these parameters in mind we choose $k_0=12$ cm^{-1} in the wiggler-type free-electron laser and adjust the value of the guide field in it, so that the transverse velocity of the beam $[u_{20}=k_0u_{30}\alpha_0/(\gamma_0 k_{0_w}u_{30}-\Omega)]$ is the same as in the electromagnetically pumped free-electron laser ($u_\perp=0.1$). On the other hand, in the electromagnetically pumped free-electron laser, we consider two possibilities $k_0=6.3$ and 5.0 cm^{-1}. The frequency ω_0' of the pump wave was chosen according to Eq. (34) so that the frequency ω' of the amplified radiation is the same in both lasers ($\omega'=180$ cm^{-1}). This choice of k_0 and ω_0' corresponds to two values of $v_p=0.85$ and 1.30. The guide field in the electromagnetically pumped laser was also adjusted so that $u_\perp=0.1$. The calculated small signal gains for the described three configurations are presented in Fig. 5, where the normalized gain parameter $\eta=10\log_{10}|\Gamma/N_eF'|$ is shown as a function of the strength of the pump field α_0. All the graphs show significant gain enhancements at certain values of α_0. The calculations show (see Fig. 6) that these critical points correspond to the conditions $\mu_0\to 0$, $\mu_s\to 0$ which physically describe the case of an enhanced induced response of the system in the vicinity of orbital instability. An additional important feature of the results shown in Fig. 5 is that the enhancement of the gain takes place at very low values of the pump field. For instance, for $v_p=1.30$ the critical $\alpha_0=1.75\times 10^{-3}$ corresponds to the magnetic component of the pump of only ~ 18 G. This salient feature is due to the resonant form of u_{20} [see (9)] which allows us to keep the value of u_{20} constant by using a small value for α_0 and, at the same time, approaching the resonance condition in the denominator. Because of the proximity to the unstable orbital regime, however, the quality of the electron beam must probably be very high in the above mentioned enhanced-response regime.

We summarize this paper as follows.

(i) The present work presents a comprehensive study of the free-electron laser in combined transverse electromagnetic pump and magnetostatic guide fields.

(ii) It was shown that several different helical steady-state stable equilibria of the beam may exist for a given beam energy and configuration of the pump and guide fields.

(iii) Stability of the helical orbits and ways of launching the beam into one of the stable steady-state orbits were discussed and illustrated in numerical examples.

(iv) A formalism for calculating the small signal single-particle gain for beams in the helical equilibria was developed. The resulting gain formula shows a possibility of an enhanced-gain regime when the laser is operated in the vicinity of unstable zero-order helical electron trajectories. A salient feature in this regime is a possibility of the gain enhancement at relatively low-power densities of the pump electromagnetic wave.

[1]L. R. Elias, Phys. Rev. Lett. **42**, 977 (1979).
[2]Y. Carmel, V. L. Granatstein, and A. Gover, Phys. Rev. Lett. **51**, 566 (1983).
[3]L. Friedland, Phys. Fluids **23**, 2376 (1980).
[4]L. Friedland and J. L. Hirshfield, Phys. Rev. Lett. **44**, 1456 (1980).
[5]P. Sprangle, V. L. Granatstein, and L. Baker, Phys. Rev. A **12**, 1697 (1975).

[6]I. B. Bernstein and L. Friedland, Phys. Rev. A **23**, 816 (1981).
[7]Y. Gell, J. R. Torstensson, and H. Wilhelmsson, and B. Levush, Appl. Phys. B **27**, 15 (1982).
[8]L. Stenflo, Phys. Scr. **21**, 831 (1980).
[9]L. Stenflo, Phys. Scr. **23**, 779 (1981).
[10]L. Stenflo and H. W. Chelmsson, Phys. Rev. A **24**, 1115 (1981).
[11]L. Friedland, Phys. Rev. A **29**, 1310 (1984).
[12]A. Fruchtman and L. Friedland, Int. J. Infrared Millimeter Waves **5**, 683 (1984).